



ChemComm

**Durable Gelfoams Stabilized by Compressible  
Nanocomposite Microgels**

|               |                          |
|---------------|--------------------------|
| Journal:      | <i>ChemComm</i>          |
| Manuscript ID | CC-COM-09-2022-004993.R1 |
| Article Type: | Communication            |
|               |                          |

SCHOLARONE™  
Manuscripts

## COMMUNICATION

## Durable Gelfoams Stabilized by Compressible Nanocomposite Microgels

Received 00th January 20xx,  
Accepted 00th January 20xx

Yuichiro Nishizawa,<sup>a,\*</sup> Takumi Watanabe,<sup>a,\*</sup> Tetsuya Noguchi,<sup>a</sup> Masaya Takizawa,<sup>a</sup> Chihong Song,<sup>c</sup> Kazuyoshi Murata,<sup>c</sup> Haruka Minato,<sup>a</sup> and Daisuke Suzuki<sup>\*a,b</sup>

DOI: 10.1039/x0xx00000x

Although hydrogel microspheres (microgels) are useful as emulsion stabilizers, typical microgels cannot stabilize foams over a prolonged period of time. Here, we found that compressible nanocomposite microgels with solid nanoparticles can overcome undesired desorption of microgels from the air/water interface of bubbles, and form highly durable, microgel-surrounded foams (gelfoams).

Aqueous foams, which are dispersions of gas bubbles in a continuous liquid phase, are ubiquitous in nature and in daily life. Based on their properties, i.e., deformability, environmental safety, and light weight, aqueous foams have been used in a wide range of applications including cosmetics, catalysis, pharmaceuticals, and energy-storage devices.<sup>1</sup> In general, aqueous foams are thermodynamically unstable systems, and thus the air/water interface must be stabilized with suitable surface-active materials, such as low-molecular-weight surfactants, polymers, or colloidal particles.<sup>2</sup>

Among these, colloidal particles promise great potential as interfacial stabilizers for both air/water and oil/water interfaces due to their higher adsorption energy at interfaces than low-molecular-weight surfactants.<sup>3</sup> In particular, hydrogel microspheres (microgels) have been studied as particulate stabilizers on account of their fascinating properties.<sup>4</sup> For instance, compared to rigid colloidal particles made of e.g., polystyrene (PS) or silica, microgels composed of amphiphilic polymers can stabilize interfaces with a lower energy input given that highly swollen microgels spontaneously adsorb at interfaces.<sup>5</sup> Moreover, the excellent biocompatibility of highly water-swollen microgels is attractive,<sup>6</sup> as it makes them suitable for applications in biomaterials. Therefore, various types of

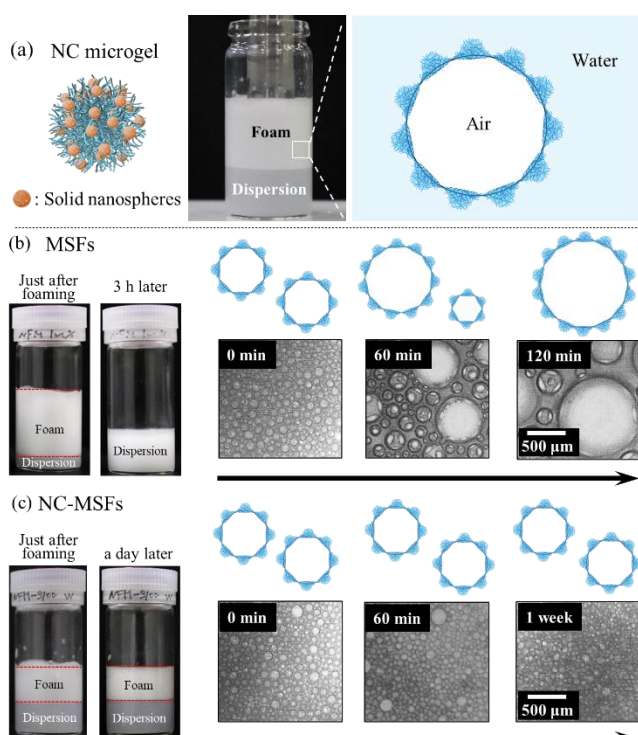


**Figure 1.** (a) Schematic illustration of a nanocomposite (NC) microgels and durable gelfoams stabilized by NC-microgels (NC-MSFs). (b) MSFs and (c) NC-MSFs prepared by mixing microgel dispersions using a homogenizer. The time-dependence of the foams and gas bubbles observed using optical microscopy.

microgels have been developed as particulate stabilizers for interfaces.<sup>4,6d,7</sup>

Although there have been various studies on microgel-stabilized emulsions,<sup>4,7</sup> the number of reports on microgel-stabilized aqueous foams (MSFs) is low.<sup>8</sup> One of the biggest problems currently associated with MSFs is their extremely low storage stability; microgels surrounding gas bubbles are easily detached from the air/water interface, resulting in coalescence and coarsening of the bubbles (Movie S1). So far, changing the surface charge,<sup>8b</sup> degree of crosslinking,<sup>8c</sup> and swelling states of microgels have been investigated in this context.<sup>8d</sup> However, to

<sup>a</sup> Graduate School of Textile Science & Technology, Shinshu University, Japan.  
E-mail: d\_suzuki@shinshu-u.ac.jp

<sup>b</sup> Research Initiative for Supra-Materials, Interdisciplinary Cluster for Cutting Edge Research Institution, Shinshu University, Japan.

<sup>c</sup> National Institute for Physiological Sciences and Exploratory Research Center on Life and Living Systems, National Institutes of Natural Sciences, Japan.

\* These authors contributed equally to this work.

Electronic Supplementary Information (ESI) available: [details of any supplementary information available should be included here]. See DOI: 10.1039/x0xx00000x

the best of our knowledge, coalescence and coarsening of gas bubbles in MSFs was always observed within a few hours at the longest.<sup>8a,c,d</sup>

In the present study, we discovered that the modification of microgels with rigid nanoparticles, i.e., nanocomposite (NC) microgels, is crucial to form MSFs with high storage stability (Figure 1). In contrast to MSFs (Figures 1b and S1a, Table S1), the obtained NC-MSFs, referred to henceforth as gelfoams, maintained their structure for more than a month (Figures 1c and S1c).

The NC microgels that can form durable gelfoams have a compressible nanostructure in which a layer of rigid nanoparticles exists near the microgel surface. Such NC microgels were developed by seeded emulsion polymerization of styrene in the presence of charged poly(*N*-isopropyl acrylamide) (pNIPAm)-based microgels (SEPM).<sup>6ad</sup> Based on our previous findings that hydrophobic monomers, such as styrene, compound in a selective manner avoiding the charged groups in the core microgels,<sup>7a,9</sup> in this study, we designed novel colloidal stable NC microgels.

First, core microgels were synthesized by precipitation polymerization using NIPAm, methacrylic acid (MAc), fumaric acid (FAc), and the crosslinker *N,N'*-methylenebis(acrylamide) (BIS) (henceforth denoted as NMF; Figure S2). It is widely accepted that MAc and FAc are located in the center and the surface of pNIPAm-based microgels prepared by precipitation polymerization, respectively, as a result of their differing monomer reactivity.<sup>9e</sup> Thus, we hypothesized that the generated NMF microgels would possess carboxyl groups located at both the center and surface of the microgels. Next, using the NMF microgels as cores, SEPM of styrene was performed to obtain NC microgels. The NC microgels were denoted as NMF-SX, where X refers to the concentration of styrene (mM) during the polymerization. FE-SEM images (Figure 2a (left)), show that NC microgels with low amounts of PS (NMF-S100) are deformed after drying on the substrates, while the spherical shape was maintained upon increasing the amount of styrene present during the polymerization (NMF-S300; Figure 2d (left)). This particle-deformation trend was also observed in TEM images of ultrathin cross sections, in which PS was stained in black using RuO<sub>4</sub> (Figure 2ad (right)); PS nanoparticles only form near the surface of the microgels, which is probably due to an attempt to avoid the polyelectrolytes inside the microgels. It should also be noted here that a pH-responsive hydrogel layer detected by electrophoresis was maintained on the surface of all the NC microgels (Table S2).

The nanostructures of the swollen NC microgels were visualized in more detail by cryo-electron tomography (cryo-EM) (Figure 2bcef). Many independent PS nanospheres were observed in NMF-S100; on the other hand, the PS nanospheres fuse to form a continuous PS thin layer in NMF-S300. The differences in nanostructure affect the swelling/deswelling behavior of the thermoresponsive pNIPAm-based microgels, as confirmed by DLS; the hydrodynamic diameter ( $D_h$ ) of NMF-S100 decreases with increasing temperature, whereas that of NMF-S300 remain almost constant upon varying temperature and pH value (Table S2).

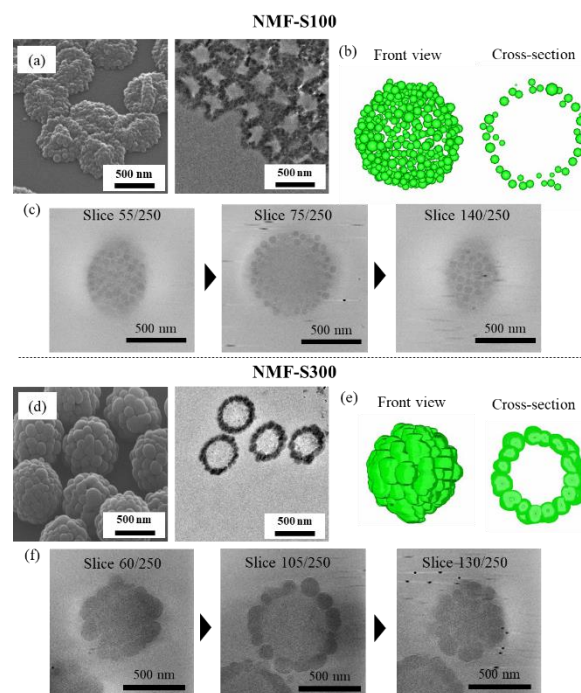


**Figure 2.** Characterization of NC microgels using different visualization techniques; (abc) NMF-S100 and (def) NMF-S300. (ad) FE-SEM images (left) and TEM images of ultra-thin cross sections (right) of NC microgels. (be) Segmentation images of NC microgels obtained by cryo-TEM characterization. (cf) Cryo-ET images of different cross-section slices. For details of the cryo-ET analysis, see movie S2 and S3.

In order to compare their foamability and storage stability, foams stabilized by modified and unmodified microgels were prepared by mixing the microgel dispersions using a homogenizer under the same operating conditions. Here, the unmodified pNIPAm-based microgels are denoted as N(x), where x is the cross-linking density, and the following number shows the particle size. Poly(*N*-isopropyl methacrylamide) (pNIPAm) microgels crosslinked with BIS were also examined as a control. As shown in Figure 1b, foams stabilized by NMF microgels completely disappeared within 3 hours. Optical microscopy revealed that the size of the gas bubbles in the unmodified MSFs increased significantly within a short period of time. Similarly, the foams stabilized by unmodified microgels with different size, cross-linking density, chemical species, charged-group distribution, and structure (core-shell) were coarsened or collapsed after less than a day (Figure S1a and f–o, Table S1). These results are also consistent with previous reports.<sup>8</sup> On the other hand, the durable gelfoams stabilized by NMF-S100 showed little collapse after one day and were maintained even after a month (Figures 1c, S1cd, S3 and S4). The gas bubbles in the durable gelfoams did not show any remarkable size change for at least a week (Figures 1bc, 3a, S5). The amount of foam just after homogenization decreased with increasing amount of immobilized PS in the NMF microgels (NMF-S200), and NMF-S300 could not stabilize the air/water interfaces in foams (Figure S1e). It should also be noted here that the foamability of NMF-S50 was almost the same as that of the unmodified NMF microgels, and the resulting foam exhibited poor storage stability (Figures S1b, S4), suggesting that there is an optimal nanocomposite structure for preparing

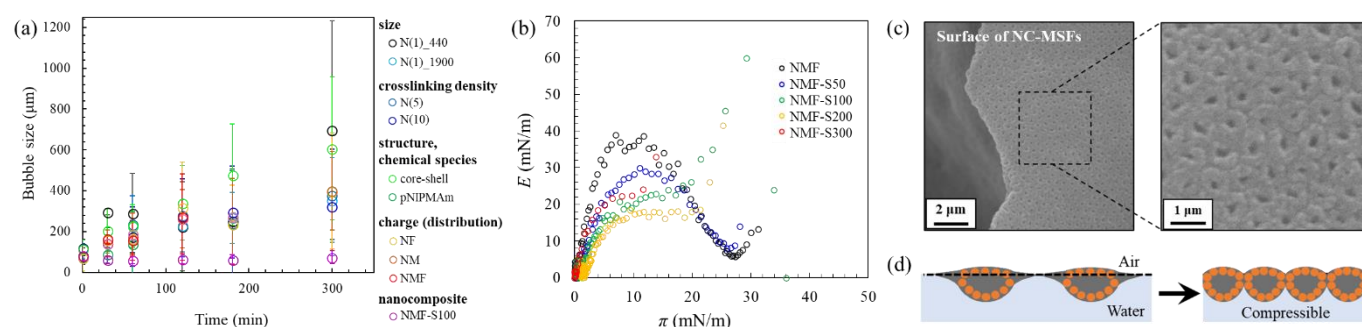


**Figure 3.** (a) Time-dependence of the bubble size in the MSFs and durable gelfoams. (b) Compression elastic modulus,  $E$ , as a function of surface pressure,  $\pi$ , at the air/water interface at 25 °C for unmodified NMF microgels and NC microgels. (c) SEM images of the obtained NMF-S100 film for different surface pressures. (d) Schematic illustration of the compression behavior of NC microgels.

durable gelfoams. NMF-S100 microgels, which were the optimal nanocomposites among those investigated, were able to create durable gelfoams under different pH conditions (pH = 3 and 11) (Figure S6), confirming that the NC nanocomposite structures, rather than the charge state, plays an important role in foam stabilization.

To investigate the reason for the high storage stability of NC-MSFs stabilized by NMF-S100 microgels, the compression elastic modulus ( $E = -d\pi/d\ln A$ , where  $\pi$  is the surface pressure and  $A$  is the normalized area defined as interfacial area / weight of microgels) of a monolayer of each microgel was investigated at the air/water interface using a Langmuir trough.<sup>10</sup>  $E$  is strongly correlated to the suppression of Ostwald ripening in foams or emulsions.<sup>11</sup> As a control experiment, for an unmodified NMF microgel monolayer, the maximum compression elastic modulus,  $E_{\max}$  (37 mN/m) was obtained at  $\pi = 7.8$  mN/m;  $E$  then decreased with increasing  $\pi$  (Figures 3b, S7), suggesting the desorption of the polymer segments on the microgels from the air/water interfaces. A similar trend was observed when the NMF-S50 microgels, which cannot stabilize gas bubbles for a long period of time, were used. Conversely, for the NMF-S100 microgels, the  $E_{\max}$  (60 mN/m) of the microgel monolayer occurred at  $\pi = 29.3$  mN/m without a decrease in  $E$  when  $\pi$  was further increased. SEM images of the surface of dried NC-MSFs on a solid substrate revealed that each NMF-S100 microgel was highly compressed in the monolayer (Figure 3cd). The rigid spherical NMF-S300 microgels also exhibited high  $E_{\max}$  (33 mN/m), but NMF-S300 could not form such gelfoams due to low surface activity of these microgels. Although further investigations are required to clarify the effect of hydrophobicity<sup>12</sup> and surface roughness<sup>13</sup> of the microgels, our present results clearly show that compressibility and microgel modification are effective for creating robust gelfoams.

The features of the obtained durable gelfoam, which was maintained for up to 4 months (Figure S8) can be summarized as follows. One of the advantages of MSFs is the ease of foam preparation, because pNIPAm is an interface-active polymer.<sup>5</sup> In contrast to foams stabilized by conventional PS particles, gelfoams stabilized by NMF-S100 can be obtained simply by shaking the dispersion by hand (Figure 4a).

Another desirable feature of the durable gelfoams is their thermal stability (Figure 4b). Harrer et al. have reported that the stimulus-responsiveness of the dangling chains of microgels

adsorbed at air/water interfaces is suppressed by decreasing their water content due to the orientation of the hydrophobic groups toward the air phase.<sup>14</sup> In addition, we have clarified that the temperature-responsiveness of microgels that are highly packed on solid/liquid interfaces is limited by the interpenetration of dangling chains and compression from neighboring microgels.<sup>15</sup> Therefore, it is possible that the thermoresponsiveness of NMF-S100 microgels is suppressed due to the effects of strong adsorption of their polymer segments onto the interfaces, compression, and the interpenetration of dangling chains.

Furthermore, the physical properties of the NC-MSFs were compared to those of unmodified MSFs and foams stabilized by solid PS. To the best of our knowledge, the physical properties of foams stabilized by microgels have not been investigated so far, probably because the MSFs are usually unstable. In this study, the physical properties of MSFs just after foaming and NC-MSFs were evaluated for the first time using dynamic viscoelastic measurements. PS-stabilized foams were prepared as a control by adding NaCl, as reported previously (Figure S9).<sup>16</sup> All foams exhibited yielding behavior (Figures 4c, S10), and the MSFs and NC-MSFs had lower maximum storage moduli ( $G'_{\max} \sim 100$  Pa) compared to the foam stabilized with PS. It is worth noting here that the gelfoams maintained their low storage elastic modulus for at least a month (Figure 4c) on account of their durability. Moreover, like those of the MSFs, the  $G'_{\max}$  values of the NC-MSFs (NMF-S100) were almost constant regardless of the NaCl concentration, whereas those of the PS-stabilized foams exhibited a strong dependence on the NaCl concentration (Figure 4d). Since NMF-S100 maintained colloidal stability even at high salt concentrations due to the polyelectrolytes at the particle surface (Figure S11), the gelfoams exhibited salt tolerance and their rheological properties did not change significantly. Thus, the durable gelfoams prepared using the optimized NC microgels are expected to be applied not only in cosmetics and catalysis, but also in bioapplications, which are often performed under high salt concentration conditions.

In conclusion, we found that durable gelfoams can be realized with nanocomposite (NC) microgels prepared by seeded emulsion polymerization of styrene in the presence of charged poly(*N*-isopropyl acrylamide) (pNIPAm)-based microgels (SEPM). The crucial stabilizers are NMF-S100 NC-

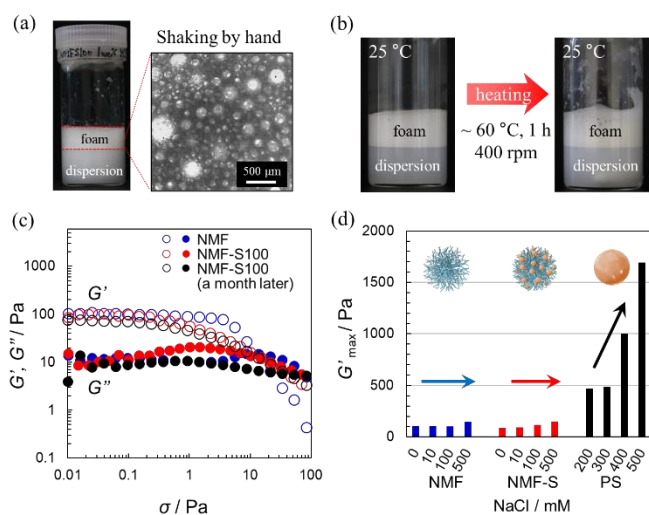


**Figure 4.** Features of gelfoams stabilized by the NC microgels. (a) Easy foamability: gelfoams could be obtained by shaking by hand. (b) Thermal tolerance: gelfoams stabilized by 1 wt% NMF-S100 (pure water) were kept at  $\sim 60$  °C for 1 hour with stirring at 400 rpm. (c) Strain dependence of the storage modulus ( $G'$ ) and loss modulus ( $G''$ ) of foams stabilized by NMF and NMF-S100. (d)  $G'_{\max}$  of foams with different ionic strength.

microgels, which contain independent PS nanospheres inside water-swollen microgels, avoiding the microgel center and surface (cf. e.g., Figure 2a). As such foams were not obtained using NMF-S300 microgels, which have a solid-like particle interface, or the parent microgels, the fabricated NC structure is a key factor for forming these durable gelfoams. The NC microgels afford high storage stability, low storage elastic modulus, and tolerance toward temperature and ionic strength. Moreover, durable gelfoams can be obtained without the use of additives other than water and NC microgels. Therefore, our findings can be expected to lead to useful applications where such foams are used e.g., at high ionic concentrations, which is often the case in biomaterials.

D.S. acknowledges a Grant-in-Aid for Exploratory Research (21K18999), a Grant-in-Aid for Scientific Research on Innovative Areas "Molecular Engine" (21H00392) from the Japan Society for the Promotion of Science (JSPS), and a CREST Grant-in-Aid (JPMJCR21L2) from the Japan Science and Technology Agency (JST). This work was also supported by JSPS KAKENHI grant 16H06280 and a Grant-in-Aid for Scientific Research on Innovative Areas - Platforms for Advanced Technologies and Research Resources ("Advanced BioImaging Support").

## Conflicts of interest

There are no conflicts to declare.

## Notes and references

- (a) B. P. Binks, R. Murakami, *Nat. Mater.* 2006, **5**, 865-869; (b) S. Fujii, *Polymer J.* 2019, **51**, 1081-1101; (c) C. Chen, J. Song, J. Cheng, Z. Pang, W. Gan, G. Chen, Y. Kuang, H. Huang, U. Ray, T. Li, L. Hu, *ACS Nano* 2020, **14**, 16723-16734; (d) Y. Yang, Z. Chu, Q. Huang, Y. Li, B. Zheng, J. Chang, Z. Yang, *J. Hazard. Mater.* 2021, **420**, 126622; (e) D. Dedover, Q. Li, L. Leclercq,

V. Nardello-Rataj, J. Leng, S. Zhao, M. Pera-Titus, *Angew. Chem. Int. Ed.* 2022, **61**, e202107537.

- (a) R. J. Pugh, *Adv. Colloid Interface Sci.* 1996, **64**, 67-142; (b) B. P. Binks, *Curr. Opin. Colloid Interface Sci.* 2002, **7**, 21-41; (c) A.-L. Fameau, S. Fujii, *Curr. Opin. Colloid Interface Sci.* 2020, **50**, 101380.
- J. Wu, G.-H. Ma, *Small* 2016, **12**, 4633-4648.
- (a) T. Ngai, S. H. Behrens, H. Auweter, *Chem. Commun.* 2005, 331-333; (b) S. Fujii, E. S. Read, B. P. Binks, S. P. Armes, *Adv. Mater.*, 2005, **17**, 1014-1018; (c) D. Suzuki, S. Tsuji, H. Kawaguchi, *J. Am. Chem. Soc.* 2007, **26**, 8088-8089; (d) S. Wiese, A. C. Spiess, W. Richtering, *Angew. Chem. Int. Ed.* 2013, **52**, 576-579.
- (a) K. Horigome, D. Suzuki, *Langmuir* 2012, **28**, 12962-12970; (b) Z. Li, D. Harbottle, E. Pensini, T. Ngai, W. Richtering, Z. Xu, *Langmuir* 2015, **31**, 6282-6288; (c) C. Buchcic, R. H. Tromp, M. B. J. Meinders, M. A. C. Stuart, *Soft Matter* 2017, **13**, 1326-1334; (d) H. Minato, M. Murai, T. Watanabe, S. Matsui, M. Takizawa, T. Kureha, D. Suzuki, *Chem. Commun.* 2018, **54**, 932-935; (e) M. Takizawa, Y. Sazuka, K. Horigome, Y. Sakurai, S. Matsui, H. Minato, T. Kureha, D. Suzuki, *Langmuir* 2018, **34**, 4515-4525; (f) H. Minato, M. Takizawa, S. Hiroshige, D. Suzuki, *Langmuir* 2019, **35**, 10412-10423.
- (a) M. Karg, A. Pich, T. Hellweg, T. Hoare, L. A. Lyon, J. J. Crassous, D. Suzuki, R. A. Gumerov, S. Schneider, I. I. Potemkin, W. Richtering, *Langmuir* 2019, **35**, 6231-6255; (b) D. Suzuki, K. Horigome, T. Kureha, S. Matsui, T. Watanabe, *Polymer J.* 2017, **49**, 695-702.
- (a) T. Watanabe, M. Takizawa, H. Jiang, T. Ngai, D. Suzuki, *Chem. Commun.* 2019, **55**, 5990-5993; (b) M.-H. Kwok, G. Sun, T. Ngai, *Langmuir* 2019, **35**, 4205-4217; (c) Y. Li, S. Zhang, H. Jiang, X. Guan, T. Ngai, *Langmuir* 2022, **38**, 6571-6578.
- (a) A. Maestro, D. Jones, C. Sánchez de Rojas Candela, E. Guzman, M. H. G. Duits, P. Cicuti, *Langmuir* 2018, **34**, 7067-7076; (b) D. Wu, V. Mihali, A. Honciuc, *Langmuir* 2019, **35**, 212-221; (c) Y. Xie, Y. Xu, J. Xu, *J. Colloid Interface Sci.* 2021, **597**, 383-392; (d) J. Xu, H. Qiao, K. Yu, M. Chen, C. Liu, W. Richtering, H. Zhang, *Chem. Eng. J.* 2022, **442**, 136274.
- (a) D. Suzuki, T. Yamagata, M. Murai, *Langmuir* 2013, **29**, 10579-10585; (b) D. Suzuki, C. Kobayashi, *Langmuir* 2014, **30**, 7085-7092; (c) C. Kobayashi, T. Watanabe, K. Murata, T. Kureha, D. Suzuki, *Langmuir* 2016, **32**, 1429-1439; (d) T. Watanabe, C. Kobayashi, C. Song, K. Murata, T. Kureha, D. Suzuki, *Langmuir* 2016, **32**, 12760-12773; (e) T. Watanabe, C. Song, K. Murata, T. Kureha, D. Suzuki, *Langmuir* 2018, **34**, 8571-8580; (f) T. Watanabe, Y. Nishizawa, H. Minato, C. Song, K. Murata, D. Suzuki, *Angew. Chem. Int. Ed.* 2020, **59**, 8849-8853.
- (a) F. Pinaud, K. Geisel, P. Massé, B. Catargi, L. Isa, W. Richtering, V. Ravaine, V. Schmitt, *Soft Matter* 2014, **10**, 6963-6974; (b) C. Picard, P. Garrigue, M.-C. Taty, V. Lapeyre, S. Ravaine, V. Schmitt, V. Ravaine, *Langmuir* 2017, **33**, 7968-7981.
- (a) M. B. J. Meinders, T. van Vliet, *Adv. Colloid Interface Sci.* 2004, **108**, 119-126; (b) D. Georgieva, A. Cagna, D. Langevin, *Soft Matter* 2009, **5**, 2063-2071.
- M. Safouane, D. Langevin, B. P. Binks, *Langmuir* 2007, **23**, 11546-11553.
- M. Zanini, C. Marschelke, S. E. Anachkov, E. Marini, A. Synytska, L. Isa, *Nat. Commun.* 2017, **8**, 15701.
- J. Harrer, M. Rey, S. Ciarella, H. Löwen, L. M. C. Janssen, N. Vogel, *Langmuir* 2019, **35**, 10512-10521.
- (a) H. Minato, Y. Nishizawa, T. Uchihashi, D. Suzuki, *Polymer J.* 2020, **52**, 1137-1141; (b) Y. Nishizawa, H. Minato, T. Inui, I. Saito, T. Kureha, M. Shibayama, T. Uchihashi, D. Suzuki, *RSC Advances* 2021, **11**, 13130-13137.
- B. P. Binks, B. Duncumb, R. Murakami, *Langmuir* 2007, **23**, 9143-9146.